

COMPARISON OF DEPTH PROFILES OF ^{129}I AND ^{14}C CONCENTRATION IN THE SURFACE LAYER OF SOILS COLLECTED FROM NORTHEASTERN JAPAN

Hiroyuki Matsuzaki^{1,2} • Yoko Sunohara Tsuchiya¹ • Yasuyuki Muramatsu³ • Yuji Maejima⁴ • Yosuke Miyairi¹ • Kazuhiro Kato⁵

ABSTRACT. $^{129}\text{I}/^{127}\text{I}$ and $^{14}\text{C}/^{12}\text{C}$ depth profiles were compared for the surface 30-cm layer of soil samples (Andisols) collected from Shimokita Peninsula, northeastern Japan, in November 2005. The $^{129}\text{I}/^{127}\text{I}$ and $^{14}\text{C}/^{12}\text{C}$ profiles have a clear correlation, even taking into account that the data include samples collected from different sites with different surface histories. These results, and considering that $^{14}\text{C}/^{12}\text{C}$ can be regarded as a proxy of the original depth in stable soil, show the diversity of the $^{129}\text{I}/^{127}\text{I}$ ratio at the surface among the sites, indicating variations in the thicknesses of the layers recently removed. At one of the sampling sites (P003-1), the $\Delta^{14}\text{C}$ value measures $\sim 110\%$ near the surface, which is indicative of anthropogenic ^{14}C produced by atmospheric testing of nuclear weapons during the late 1950s and early 1960s. This site has experienced no disturbances for at least the past 50 yr. The relatively high activity of ^{129}I (0.8 mBq/kg) and the $^{129}\text{I}/^{127}\text{I}$ ratio (7×10^{-9}) observed at the top layer of this site can be considered a “representative value” when considering the anthropogenic iodine transfer from the atmosphere to the ground. The observations also support 2 separate modes of ^{129}I migration in the soil: i.e. “topmost quick diffusion” and “subsurface relatively slow migration process.” Even in the “subsurface relatively slow migration zone,” the $^{129}\text{I}/^{127}\text{I}$ ratio was still orders higher than the pre-anthropogenic natural level.

INTRODUCTION

By means of accelerator mass spectrometry (AMS), the $^{129}\text{I}/^{127}\text{I}$ isotope system becomes an entirely new tool for Earth environmental analysis. AMS is at least several orders more sensitive in terms of the detection limit of ^{129}I compared with other methods, including neutron activation analysis (NAA). From the new perspective provided by ^{129}I AMS, a wide range of ^{129}I distributions in the Earth’s surface layer has been revealed. Most of the ^{129}I present in the Earth’s surface today was produced artificially by nuclear activities such as nuclear weapons testing and nuclear power generation. After treaties put an end to the bomb testing, nuclear fuel reprocessing plants became the major source of environmental ^{129}I . Many articles have reported high ^{129}I concentrations in the vicinity of nuclear fuel reprocessing plants (e.g. Yiou et al. 1994; Moran et al. 1999). Although the number is limited, careful studies have evaluated the natural level of $^{129}\text{I}/^{127}\text{I}$ before human nuclear activities as at most 1.5×10^{-12} (e.g. Moran et al. 1998).

A recent investigation in Japan (Muramatsu et al. 2008) has found significantly higher $^{129}\text{I}/^{127}\text{I}$ ratios compared to the natural level even on land surfaces far from nuclear facilities. They measured the concentration of ^{129}I and ^{127}I in several surface soil samples collected from various regions in Japan and reported the range of $^{129}\text{I}/^{127}\text{I}$ from 3.9×10^{-11} to 2.2×10^{-8} , levels that are much higher than the estimated natural level of 1.5×10^{-12} . The diversity in the data is due to the soil type, the type of land use (forest, crop field, rice paddy, etc.), and surface disturbances by natural and/or artificial means.

^{129}I generally arrives to the land surface from the atmosphere and should diffuse or penetrate into the soil. Quantitative investigation of these processes is crucial when considering the dynamics of ^{129}I as well as elemental iodine in the Earth’s surface reservoirs. The key properties are the representa-

¹Department of Nuclear Engineering and Management, School of Engineering, University of Tokyo, Hongo 7-3-1, Bunkyo-ku, Tokyo 113-8656, Japan.

²Corresponding author: Email address: hmatsu@n.t.u-tokyo.ac.jp.

³Department of Chemistry, Gakushuin University, Tokyo, Japan.

⁴National Institute for Agro-Environmental Sciences, 3-1-3 Kannondai, Tsukuba 305-8604, Japan.

⁵National Institute for Environment Studies, 16-2 Onogawa, Tsukuba-City, Ibaraki 305-8506 Japan.

tive value for the ^{129}I level (or $^{129}\text{I}/^{127}\text{I}$ ratio) at the surface and the depth profile (subsurface gradient) without surface disturbance. However, it is generally difficult to evaluate the degree of surface disturbance. One way is to examine the geomorphology and the surface conditions carefully and select a point where it appears to have remained undisturbed for a long time. However, this is rather difficult because it depends on one's experience and whether the land use history is available.

Alternatively, we propose here a more direct method to utilize radiocarbon. The modern $^{14}\text{C}/^{12}\text{C}$ ratio in the atmosphere is well known and the level at the soil surface should be equilibrated with the atmosphere. Thus, it is possible to know directly whether the surface had been disturbed or not by using the $\Delta^{14}\text{C}$ value at the surface. Moreover, since $\Delta^{14}\text{C}$ generally has a clear correlation with depth, it may tell us how thick a recently removed layer was. In this study, depth profiles of both $^{129}\text{I}/^{127}\text{I}$ and $^{14}\text{C}/^{12}\text{C}$ in the surface layer of several soil samples were measured and compared.

In various aspects, iodine has a close association with organic carbon. Detailed examination of the depth profiles of $^{129}\text{I}/^{127}\text{I}$ and $^{14}\text{C}/^{12}\text{C}$ might provide new information about the relationship between iodine and carbon in soil.

SAMPLING AND EXPERIMENTAL

All soil samples were collected from Shimokita Peninsula, Aomori Prefecture, located in the north-eastern region of the Japanese main island. There is a commercial waste fuel reprocessing plant also on the Shimokita Peninsula, at Rokkasho village, and the plant is now (2009) in active test operation. However, our sampling was held in November 2005, well before the active test operation, so no influence from the reprocessing plant should have occurred. The map in Figure 1 shows the relative positions of the 4 sampling points and the reprocessing plant. Every sampling point is not far from towns and some influence of human activities should exist.

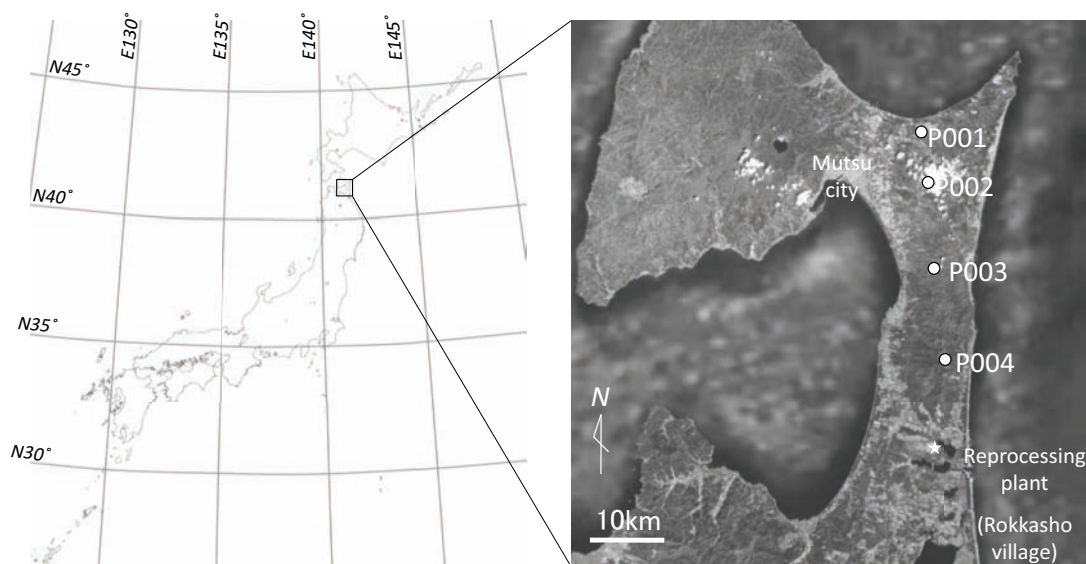


Figure 1 Sampling areas (Shimokita Peninsula, NE Japan) and their relative position to the nuclear fuel reprocessing plant

The top 30 cm of the soil surface layer was taken at each sampling point by a handheld core sampler with an inner diameter of 5 cm. The bedrock of these areas was formed by marine sediments in the

Tertiary or Quaternary. However, the “mother material” of the soil is volcanic ash deposited onto the bedrock. The soil type of all samples is classified as volcanic ash soil (Andisol), except for one that seems to be somewhat pseudogleyed with iron and manganese mottles. In total, 7 cores from 4 sampling sites were collected. Sample descriptions are summarized in Table 1.

Table 1 Soil type and sampling site description.

Site	Core ID	Core length (cm)	Soil type	Sampling site description
P001	P001-1	25.5	Andisol, brown forest soil-like	Artificially flattened surface. The P001-2 core was collected at the margin of coniferous woods. P001-1 and -2 were ~10 m apart.
	P001-2	26.5		
P002	P002-1	26.5	Pseudogleyed brown forest soil	<i>Miscanthus</i> grass land near the coniferous woods. A small fluvial system appears occasionally when it rains. It should have often been in a reduced condition.
P003	P003-1	28.5	Andisol, brown forest soil-like	Coniferous forest environment. There is an unpaved road ~5 m from the sampling sites. The undergrowth is <i>Sasa</i> type grass.
	P003-2	28.0		
P004	P004-1	28.0	Andisol, brown forest soil-like	<i>Sasa</i> grassland on a gentle slope. The P004-2 coring failed so that the core length was somewhat shortened.
	P004-2	13.0		

Each core was cut into several parts at certain intervals. The experimental procedure is summarized in Figure 2. Each soil sample was first air-dried then dried at 80 °C in an oven for several hours. The dried sample was crushed and sieved after removing litter, roots, and rocks to get a homogenized sample. From each homogenized sample, about 1 g was used for analyses of stable iodine (^{127}I) and ^{129}I . The sample was heated in a quartz tube and the evaporated iodine was collected in a trap solution. An aliquot of the solution was used to determine the stable iodine concentration by inductively coupled plasma mass spectrometry (ICP-MS) at Gakushuin University with an Agilent model 7500 ICP-MS. From the rest of the trap solution, the iodine fraction was separated by solvent extraction. Details of the stable iodine analysis and the pretreatment procedure for ^{129}I AMS are described in Muramatsu et al. (2008). $^{129}\text{I}/^{127}\text{I}$ measurements were performed at the MALT-AMS facility, University of Tokyo (Matsuzaki et al. 2007a). From each homogenized sample, 5–10 mg was taken for carbon content analysis performed with an NC analyzer at the University Museum, University of Tokyo. Depending on the carbon content, 20 to 200 mg was taken for ^{14}C AMS measurement. These samples were combusted to carbon dioxide, purified, and graphitized. $^{14}\text{C}/^{12}\text{C}$ measurements were also performed at the MALT-AMS facility, University of Tokyo (Matsuzaki et al. 2007b).

RESULTS

Measurement results are listed in Table 2. The distribution of carbon (C) content is scattered among cores. However, P001-1, P001-2, and P002-1 have a C content that is rather constant with depth. P003-1 and P003-2 have a decreasing trend in carbon content near the surface. For P004-1 and -2, the carbon content is randomly distributed.

The depth profile of stable iodine (^{127}I) concentration shows a constant trend except for in P004-1, P004-2, and the bottom of P003-1. For P004-1 and -2, the trend varies randomly with depth. Also, the bottom of P003-1 (26 cm depth) shows exceptionally high iodine concentration.

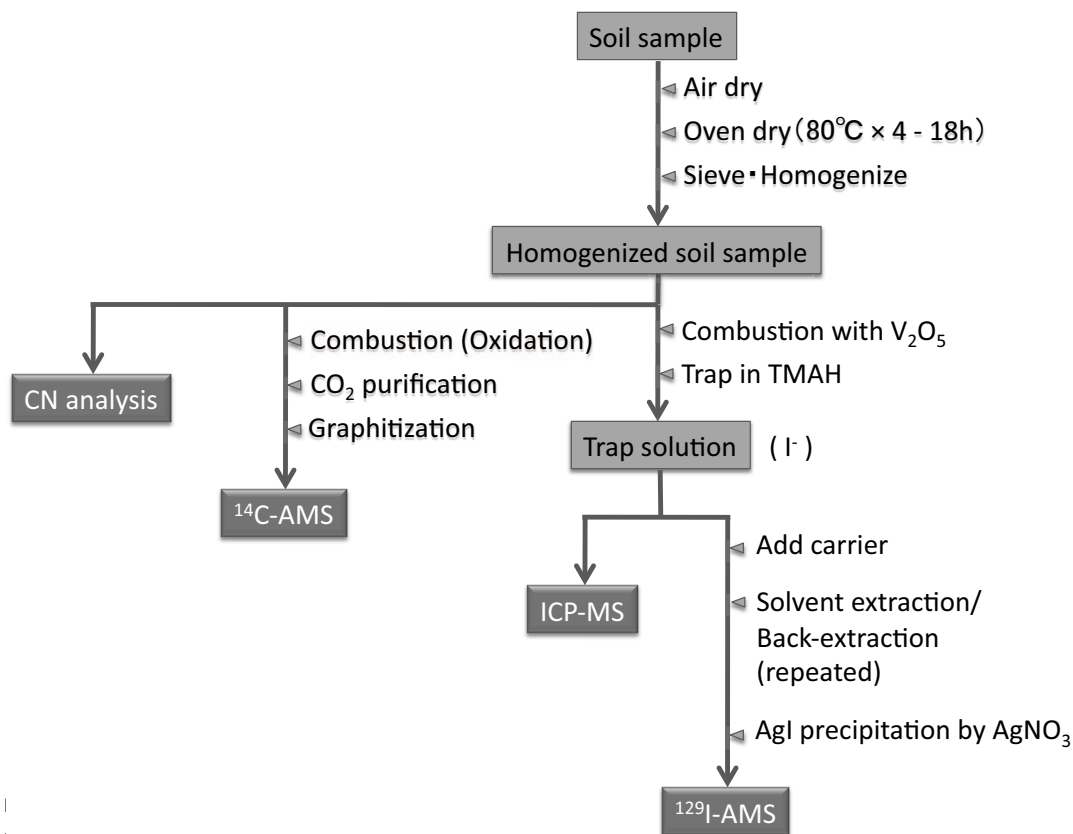


Figure 2 Pretreatment procedure for each measurement

The scattered distribution of stable iodine concentration may be partly caused by the somewhat unstable yield in the iodine extraction process due to incomplete soil homogenization. Since the iodine carrier for the AMS measurement was added after the trap in the alkaline solution, the obtained $^{129}\text{I}/^{127}\text{I}$ ratio should represent that of the original soil sample. The iodine carrier we used intrinsically has a $^{129}\text{I}/^{127}\text{I}$ ratio of 1.7×10^{-13} . $^{129}\text{I}/^{127}\text{I}$ ratios in Table 2 are already corrected for this.

The $^{129}\text{I}/^{127}\text{I}$ ratio is highest at the top of every core and decreases with depth (Figure 3). At the deepest part of these cores, the measured $^{129}\text{I}/^{127}\text{I}$ ratio (raw AMS measurements) approaches $\sim 5 \times 10^{-13}$, which is still significantly higher than the carrier value. $^{129}\text{I}/^{127}\text{I}$ ratios at the surface among cores vary widely, ranging from 5×10^{-10} (P001-1) to 7×10^{-9} (P003-1).

$^{14}\text{C}/^{12}\text{C}$ ratios are typically highest at the top and decrease with depth, except for in P001-1, P001-2, and P004-1 (Figure 4). The value near the surface of the P003-1 core exceeds that of “modern carbon,” which is a sign of nuclear weapons testing. The surface layer of P003-1 should have been undisturbed for at least 50 yr. Other cores clearly show lower $^{14}\text{C}/^{12}\text{C}$ values at their surfaces, which indicates recent removal of the surface layer to a certain thickness. P001-1, P001-2, and a part of P004-1 strangely show an increasing trend with depth.

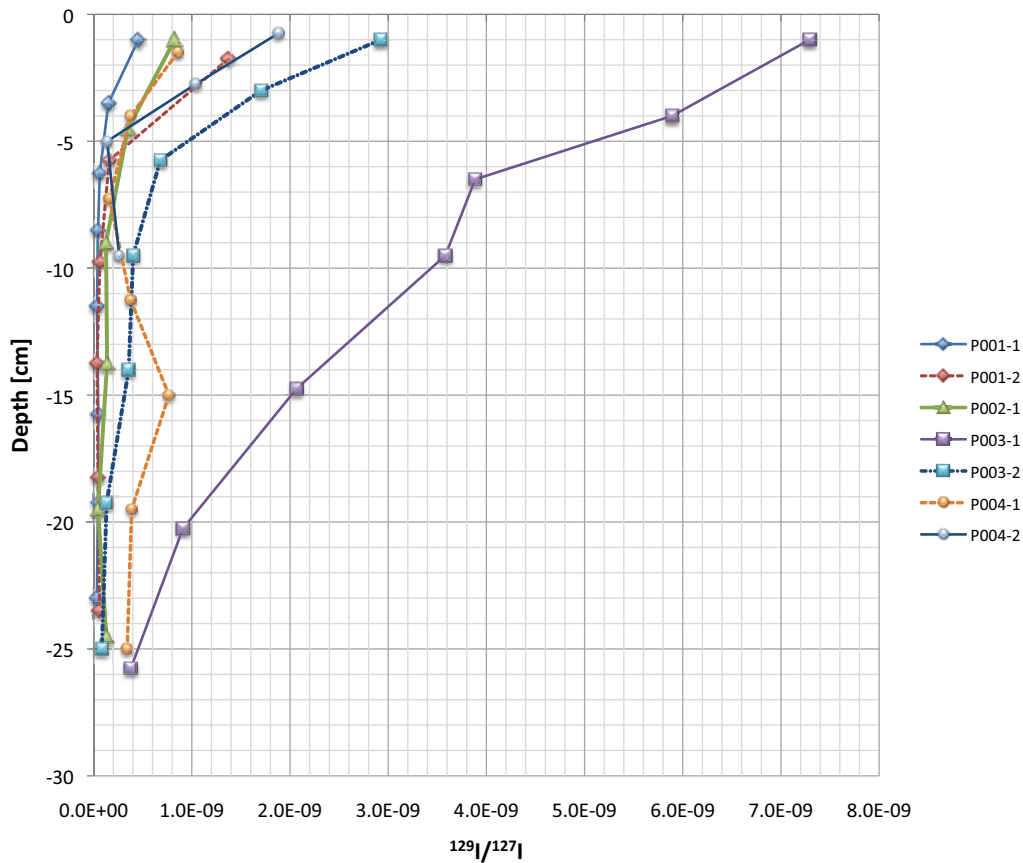
Table 2 Summary of measurement results.

Sample code	Depth (cm)	Iodine measurements				Carbon measurements	
		^{127}I content in sample ^a (ppm)	^{129}I AMS result ^b (10^{-12})	$^{129}\text{I}/^{127}\text{I}$ in sample ^c	^{129}I activity (Bq/kg)	Uncertainty for ^{129}I activity ^d	$^{14}\text{C}/^{12}\text{C}$: fraction to modern carbon ^e
P001-1-1	-1.0 ± 1.0	31.8	6.68 ± 0.16	4.56E-10	9.47E-05	3.9%	0.383 ± 0.003
P001-1-2	-3.5 ± 1.5	29.6	2.15 ± 0.06	1.51E-10	2.91E-05	4.0%	0.335 ± 0.012
P001-1-3	-6.25 ± 1.3	29.0	0.98 ± 0.03	6.27E-11	1.19E-05	4.0%	0.300 ± 0.002
P001-1-4	-8.5 ± 1.0	34.1	0.86 ± 0.02	4.49E-11	1.00E-05	4.1%	0.365 ± 0.008
P001-1-5	-11.5 ± 2.0	31.7	0.65 ± 0.02	3.40E-11	7.04E-06	4.2%	0.534 ± 0.008
P001-1-6	-15.75 ± 2.3	42.2	1.06 ± 0.03	4.75E-11	1.31E-05	4.1%	0.589 ± 0.004
P001-1-7	-19.25 ± 1.3	41.8	0.99 ± 0.03	4.41E-11	1.21E-05	4.1%	0.678 ± 0.004
P001-1-8	-23.0 ± 2.5	45.8	0.84 ± 0.02	3.31E-11	9.91E-06	4.2%	
P001-2-1	-1.75 ± 1.8	44.7	27.00 ± 0.68	1.38E-09	4.02E-04	3.9%	0.653 ± 0.003
P001-2-2	-5.75 ± 2.3	49.5	3.58 ± 0.09	1.59E-10	5.16E-05	4.0%	0.690 ± 0.010
P001-2-3	-9.75 ± 1.8	50.5	1.60 ± 0.05	6.46E-11	2.13E-05	4.2%	0.699 ± 0.006
P001-2-4	-13.75 ± 2.3	38.3	0.75 ± 0.03	3.44E-11	8.61E-06	5.0%	0.694 ± 0.005
P001-2-5	-18.25 ± 2.3	47.8	1.12 ± 0.04	4.50E-11	1.40E-05	4.5%	0.718 ± 0.004
P001-2-6	-23.5 ± 3.0	36.7	1.20 ± 0.08	6.09E-11	1.46E-05	6.9%	0.743 ± 0.005
P002-1-1	-1.0 ± 1.0	11.1	4.32 ± 0.06	8.26E-10	6.00E-05	3.3%	0.913 ± 0.011
P002-1-2	-4.5 ± 2.5	10.3	1.76 ± 0.04	3.49E-10	2.35E-05	3.7%	0.858 ± 0.006
P002-1-3	-9.0 ± 2.0	8.5	0.65 ± 0.04	1.26E-10	7.04E-06	7.1%	0.731 ± 0.004
P002-1-4	-13.75 ± 2.8	8.3	0.68 ± 0.02	1.37E-10	7.41E-06	4.5%	0.659 ± 0.004
P002-1-5	-19.5 ± 3.0	6.0	0.29 ± 0.02	4.48E-11	1.74E-06	7.8%	0.572 ± 0.003
P002-1-6	-24.5 ± 2.0	6.6	0.56 ± 0.03	1.30E-10	5.63E-06	5.5%	0.555 ± 0.003
P003-1-1	-1.0 ± 1.0	22.6	54.27 ± 8.01	7.29E-09	7.96E-04	15.1%	1.110 ± 0.010
P003-1-2	-4.0 ± 2.0	22.6	38.34 ± 2.60	5.89E-09	5.62E-04	7.4%	1.104 ± 0.007
P003-1-3	-6.5 ± 0.5	13.6	20.09 ± 1.14	3.89E-09	2.90E-04	6.4%	1.093 ± 0.005
P003-1-4	-9.5 ± 2.5	14.1	14.71 ± 0.74	3.58E-09	2.16E-04	5.8%	1.088 ± 0.005
P003-1-5	-14.75 ± 2.8	16.7	6.65 ± 0.39	2.07E-09	9.57E-05	6.6%	1.009 ± 0.007
P003-1-6	-20.25 ± 2.8	16.8	4.89 ± 0.71	9.11E-10	6.96E-05	14.9%	0.905 ± 0.006
P003-1-7	-25.75 ± 2.8	115.5	11.19 ± 0.54	3.80E-10	1.66E-04	5.7%	0.817 ± 0.011

Table 2 Summary of measurement results. (*Continued*)

Sample code	Depth (cm)	Iodine measurements				Carbon measurements	
		^{127}I content in sample ^a (ppm)	^{129}I AMS result ^b (10^{-12})	$^{129}\text{I}/^{127}\text{I}$ in sample ^c	^{129}I activity (Bq/kg)	Uncertainty for ^{129}I activity ^d	$^{14}\text{C}/^{12}\text{C}$: fraction C content (wt%) to modern carbon ^e
P003-2-1	-1.0 \pm 1.0	43.6	56.48 \pm 0.34	2.93E-09	8.35E-04	3.1%	5.10 0.981 \pm 0.005
P003-2-2	-3.0 \pm 1.0	35.6	14.83 \pm 0.12	1.71E-09	2.16E-04	3.1%	3.86 0.986 \pm 0.005
P003-2-3	-5.75 \pm 1.8	52.4	9.34 \pm 0.10	6.80E-10	1.34E-04	3.2%	3.32 0.892 \pm 0.005
P003-2-4	-9.5 \pm 2.0	63.9	7.36 \pm 0.09	4.03E-10	1.06E-04	3.2%	3.55 0.829 \pm 0.004
P003-2-5	-14.0 \pm 2.5	42.8	5.10 \pm 0.21	3.57E-10	7.33E-05	5.2%	2.22 0.728 \pm 0.011
P003-2-6	-19.25 \pm 2.8	40.4	0.95 \pm 0.02	1.32E-10	1.16E-05	3.9%	3.12 0.707 \pm 0.004
P003-2-7	-25.0 \pm 3.0	39.7	1.66 \pm 0.03	8.37E-11	2.17E-05	3.6%	2.91 0.673 \pm 0.007
P004-1-1	-1.5 \pm 1.5	14.6	5.64 \pm 0.19	8.56E-10	8.18E-05	4.5%	6.45 0.850 \pm 0.005
P004-1-2	-4.0 \pm 1.0	12.3	2.23 \pm 0.08	3.78E-10	3.03E-05	4.7%	4.28 0.777 \pm 0.006
P004-1-3	-7.25 \pm 2.3	83.2	6.04 \pm 0.20	1.62E-10	8.81E-05	4.5%	5.04 0.767 \pm 0.004
P004-1-4	-11.25 \pm 1.8	54.5	9.13 \pm 0.43	3.77E-10	1.34E-04	5.6%	6.76 0.859 \pm 0.005
P004-1-5	-15.0 \pm 2.0	9.2	3.26 \pm 0.13	7.67E-10	4.59E-05	4.9%	6.64 0.919 \pm 0.008
P004-1-6	-19.5 \pm 2.5	43.0	7.41 \pm 0.26	3.87E-10	1.09E-04	4.6%	6.61 0.858 \pm 0.005
P004-1-7	-25.0 \pm 3.0	43.1	6.58 \pm 0.22	3.42E-10	9.64E-05	4.5%	5.85 0.792 \pm 0.004
P004-2-1	-0.75 \pm 0.8	38.9	32.19 \pm 1.26	1.88E-09	4.79E-04	4.9%	4.05 0.931 \pm 0.005
P004-2-2	-2.75 \pm 1.3	40.4	18.95 \pm 0.62	1.04E-09	2.75E-04	4.4%	3.11 0.793 \pm 0.005
P004-2-3	-5.0 \pm 1.0	108.9	6.50 \pm 0.22	1.38E-10	9.84E-05	4.5%	4.76 0.771 \pm 0.004
P004-2-4	-9.5 \pm 3.5	34.4	4.15 \pm 0.14	2.60E-10	5.84E-05	4.6%	1.48 0.794 \pm 0.006

^aTypical error for ICP-MS is $\sim 3\%$.^bAll ^{129}I AMS measurements listed here were performed with 2.0 mg iodine carrier.^cUncertainty for $^{129}\text{I}/^{127}\text{I}$ in sample is determined by the error of AMS measurement.^dUncertainty for ^{129}I activity includes those of ICP-MS and AMS.^eA blank space (at P001-1-5) is due to measurement failure.

Figure 3 $^{129}\text{I}/^{127}\text{I}$ depth profiles

DISCUSSION

In every core, the $^{129}\text{I}/^{127}\text{I}$ depth profile has a generally decreasing trend with depth, with the highest ratio at the surface. After detailed observation, this decreasing profile seems to consist of 2 different trends as shown in Figure 5a, i.e. a steep gradient part nearest the surface and a relatively constant baseline. They may correspond to 2 modes of migration of ^{129}I . In recent years, ^{129}I has been deposited from the atmosphere. The amount of deposited iodine is small, but the $^{129}\text{I}/^{127}\text{I}$ ratio should be several orders higher than the general isotopic ratio in the soil. Thus, the situation can be regarded as only ^{129}I transfers from the atmosphere to the soil surface. This ^{129}I fraction migrates somewhat physically into a subsurface layer, e.g. carried in the aqueous phase, moving by capillary effect, etc. This fraction has not yet been chemically homogenized with the intrinsically existing iodine fraction in the soil and it moves quickly. This quick, physical process should cause a steep gradient profile just below the surface. During this upper process, a certain portion of ^{129}I will be absorbed gradually into the intrinsic iodine component in the soil, resulting in an increase of the $^{129}\text{I}/^{127}\text{I}$ ratio. This intrinsic component, possibly sticking to organic matter chemically, exchanges itself randomly between neighboring layers, causing a relatively slower downward movement of ^{129}I , i.e. the isotopic diffusion process. This second diffusion process should lead to the baseline depth profile of $^{129}\text{I}/^{127}\text{I}$.

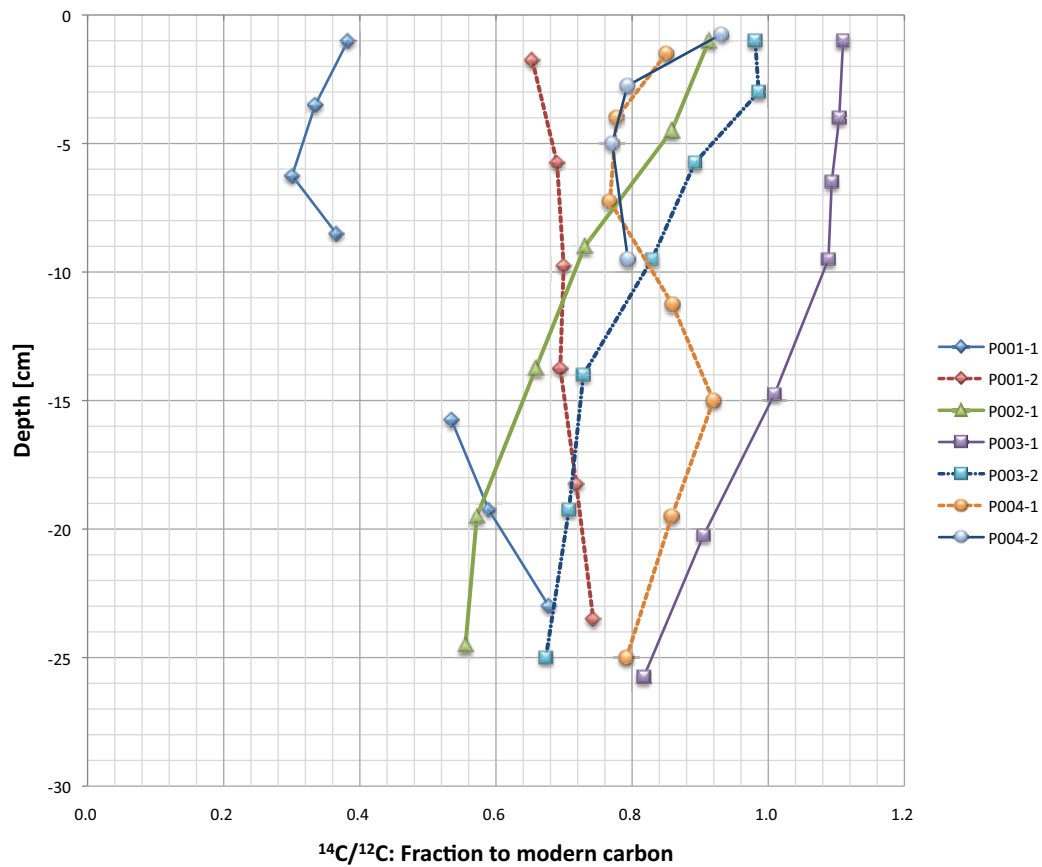


Figure 4 $^{14}\text{C}/^{12}\text{C}$ depth profiles

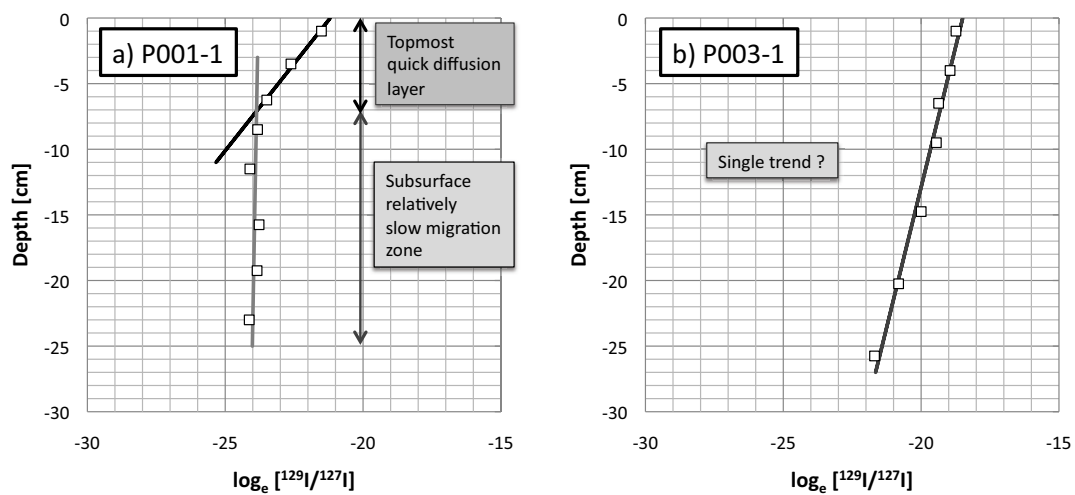


Figure 5 Details of $^{129}\text{I}/^{127}\text{I}$ depth profiles. For a) P001-1, there are 2 trends, a steep profile near the surface and a relatively constant profile. In the case of b) P003-1, there is only a single trend.

In any case, based on such penetration and diffusion processes of ^{129}I , and supposing a constant influx of ^{129}I from the atmosphere, the $^{129}\text{I}/^{127}\text{I}$ ratio at the surface gradually increases until it reaches a steady state with a constant surface $^{129}\text{I}/^{127}\text{I}$ ratio and a rather constant gradient. P003-1 is thought to be such a case (Figure 5b).

Diversity in the $^{129}\text{I}/^{127}\text{I}$ ratio at the surface is due to surface disturbance. A lower $^{129}\text{I}/^{127}\text{I}$ ratio at the surface means there has been a short duration since the fresh surface has appeared. In other words, a layer has recently been removed. The extent of the removed layer thickness would affect the degree in the drop of the surface $^{129}\text{I}/^{127}\text{I}$ ratio. Sampling point 1 has a very flat surface and it seems that it had been recently flattened. The surface $^{129}\text{I}/^{127}\text{I}$ ratios of P001-1 and P001-2 differ by a factor of 2 even though the samples are only 10 m apart. This should be attributed to the difference in thickness of the recently removed layer.

The $^{14}\text{C}/^{12}\text{C}$ profile may serve as an estimation of the surface history. The atmospheric $^{14}\text{C}/^{12}\text{C}$ ratio is well known and should be equilibrated with the stable soil surface. Generally, fresh carbon is added to the soil at the top surface by litter. Carbon then moves downward gradually during development, so that the soil gets older as it goes deeper. Simultaneously, a volatile component is dissolved and escapes as carbon dioxide gas. Consequently, the $^{14}\text{C}/^{12}\text{C}$, as well as carbon content, has a decreasing trend with depth in a stable environment. Although the detailed profile depends on the soil type and environment, the surface $^{14}\text{C}/^{12}\text{C}$ ratio and the decreasing trend are clear. This means that the $^{14}\text{C}/^{12}\text{C}$ value can serve as a proxy of the depth. Thus, we can estimate the original depth of the present surface after removal of the upper layer.

Figure 4 shows a comparison of $^{14}\text{C}/^{12}\text{C}$ depth profiles for each core measured in this study. The $^{14}\text{C}/^{12}\text{C}$ value near the surface of P003-1 shows ~10% excess over “modern carbon,” signalling the nuclear weapons test peak. Unusually excessive ^{14}C was produced by the atmospheric testing of nuclear weapons during the late 1950s and early 1960s, resulting in a ^{14}C spike with a peak $\Delta^{14}\text{C}$ value of over 800‰ in 1965 and exponentially decreasing thereafter (Bruun et al. 2005). To what extent this pulse-like spike (the “bomb spike”) had been reflected depends completely on the turnover time of soil carbon. With very quick turnover conditions as in tropical regions, the $\Delta^{14}\text{C}$ value at the soil surface is easily equilibrated with the atmosphere (Trumbore et al. 1995). In other conditions, in temperate zones such as Japan, a “bomb spike” had not been completely reflected, but a somewhat moderate increase occurs in $\Delta^{14}\text{C}$ from the surface layer of the soil (e.g. Katsuno et al. 2010). A detailed depth profile in the Japanese soil affected by the “bomb spike” had not been well studied. In a well-preserved Andisol in the controlled area of the National Institute for Agro-Environmental Sciences, Tsukuba, Japan, we observed a maximum value of 100‰ of $\Delta^{14}\text{C}$ just below the surface (Matsuzaki, unpublished data), which coincides with the result of P003-1 in this study. This means that the surface of P003-1 has been undisturbed for long time, at least 50 yr, and the ^{129}I transfer and migration process should be in a steady state, which is consistent with the discussion of the $^{129}\text{I}/^{127}\text{I}$ profile. Hence, the surface ^{129}I level (0.8 mBq/kg soil) or $^{129}\text{I}/^{127}\text{I}$ (7×10^{-9}) is, in a sense, can be considered the “representative value” for this area. P002-1 and P003-2 also show a decreasing trend, but the surface value is lower. At these locations, a certain thickness must have been removed recently, but the remaining layer was not disturbed. In the case of P001-1 and -2, the increasing trend of the $^{14}\text{C}/^{12}\text{C}$ depth profile suggests that part of these cores would have been dug up from a certain depth and piled on the surface inversely. P004-1 does not show a simple trend, which would reflect the complicated history of this site. The situation of P004-2 may be the same as P004-1 from a profile of only 10 cm. In either case, the surface value is significantly lower than the modern carbon, indicating surface disturbance.

Although the $^{129}\text{I}/^{127}\text{I}$ and $^{14}\text{C}/^{12}\text{C}$ depth profiles are fairly diverse core-to-core, these 2 parameters seem to have a clear correlation (Figure 6). Their general correlation trend indicates that the original $^{129}\text{I}/^{127}\text{I}$ profile (of “subsurface relatively static zone”), at the original depth before any surface disturbance, has been preserved. We can also find that some of the deviating points from the general trend correspond to the “topmost quick diffusion layer” of ^{129}I near the present surface. These observations support 2 different modes for the ^{129}I migration process.

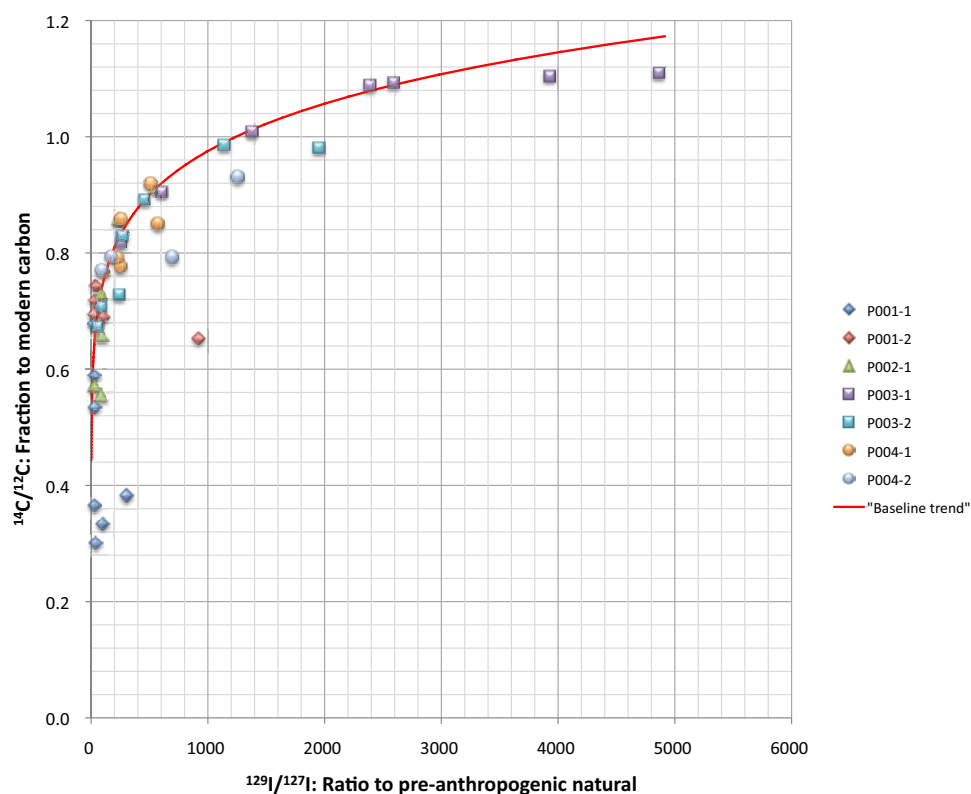


Figure 6 $^{129}\text{I}/^{127}\text{I}$ versus $^{14}\text{C}/^{12}\text{C}$. Data points form a baseline trend with some deviation points

CONCLUSION

$^{129}\text{I}/^{127}\text{I}$ and $^{14}\text{C}/^{12}\text{C}$ depth profiles were measured and compared for the surface 30-cm layer of soil samples collected from Shimokita Peninsula, northeastern Japan, in November 2005. All of these soils were classified as volcanic ash soil (Andisol).

$^{129}\text{I}/^{127}\text{I}$ and $^{14}\text{C}/^{12}\text{C}$ had a clear correlation, even when taking into account that the data include samples collected from different sites. From these results, and considering that $^{14}\text{C}/^{12}\text{C}$ can be regarded as a proxy of the original depth in stable soil, the diversity of the $^{129}\text{I}/^{127}\text{I}$ ratio at the surface among the sites indicated a variety of thicknesses of recently removed layers. At the sampling site P003-1, the $\Delta^{14}\text{C}$ value ($\sim 110\text{‰}$) near the surface was indicative of an anthropogenic origin, although this site has experienced no disturbances for at least the past 50 yr. The relatively high activity of ^{129}I (0.8 mBq/kg) and the $^{129}\text{I}/^{127}\text{I}$ ratio (7×10^{-9}) observed at the top layer of P003-1 can be considered representative values when considering the anthropogenic iodine transfer from the atmosphere to the Earth surface.

From studying the relationship between $^{129}\text{I}/^{127}\text{I}$ and $^{14}\text{C}/^{12}\text{C}$, it was observed that points near the surface of each core deviated a little from the baseline trend. These deviating points correspond to the “topmost quick diffusion layer” of ^{129}I and the others on the baseline trend correspond to the “subsurface relatively slow migration zone” that occurred in the intrinsically existing iodine. The observation supports 2 separate modes of ^{129}I migration in the soil.

Even in the “subsurface relatively slow migration zone,” the $^{129}\text{I}/^{127}\text{I}$ ratio is several orders higher than the pre-anthropogenic natural level. It would be very interesting to investigate deeper layers.

ACKNOWLEDGMENTS

The authors fully appreciate Ms Yuko Kubota, Ms Ai Sugawara, and Ms Kyoko Abe for chemical treatments carried out for the ^{129}I AMS measurements. The authors also thank Prof Kunio Yoshida and Ms Yumiko Miyazaki, at the University Museum, University of Tokyo, for the CN analysis.

REFERENCES

- Bruun S, Six J, Jensen LS, Paustian K. 2005. Estimating turnover of soil organic carbon fractions based on radiocarbon measurements. *Radiocarbon* 47(1):99–113.
- Katsuno K, Miyairi Y, Tamura K, Matsuzaki H, Fukuda K. 2010. A study of the carbon dynamics of Japanese grassland and forest using ^{14}C and ^{13}C . *Nuclear Instruments and Methods in Physics Research B* 268(7–8):1106–9.
- Matsuzaki H, Muramatsu Y, Kato K, Yasumoto M, Nakano C. 2007a. Development of ^{129}I -AMS system at MALT and measurements of ^{129}I concentrations in several Japanese soils. *Nuclear Instruments and Methods in Physics Research B* 259(1):721–6.
- Matsuzaki H, Nakano N, Tsuchiya YS, Kato K, Maejima Y, Miyairi Y, Wakasa S, Aze T. 2007b. Multi-nuclide AMS performances at MALT. *Nuclear Instruments and Methods in Physics Research B* 259(1):36–40.
- Moran JE, Fehn U, Teng RTD. 1998. Variations in $^{129}\text{I}/^{127}\text{I}$ ratios in recent marine sediments: evidence for a fossil organic component. *Chemical Geology* 152(1):193–203.
- Moran JE, Oktay S, Santschi PH, Schink DR. 1999. Atmospheric dispersal of ^{129}I from nuclear fuel reprocessing facilities. *Environmental Science & Technology* 33(15):2536–42.
- Muramatsu Y, Takada Y, Matsuzaki H, Yoshida S. 2008. AMS analysis of ^{129}I in Japanese soil samples collected from background areas far from nuclear facilities. *Quaternary Geochronology* 3(3):291–7.
- Trumbore SE, Davidson EA, Camargo PB, Nepstad DC, Martinelli LA. 1995. Belowground cycling of carbon in forests and pastures of eastern Amazonia. *Global Biogeochemical Cycles* 9(4):515–28.
- Yiou F, Raisbeck GM, Zhou ZQ, Kilian LR. 1994. ^{129}I from nuclear fuel reprocessing: potential as an oceanographic tracer. *Nuclear Instruments and Methods in Physics Research B* 92(1–4):436–9.